

On a fusion chain reaction via suprathermal ions in high-density H-¹¹B plasma

Fabio Belloni

European Commission, Directorate-General for Research and Innovation, Euratom Research, Brussels, Belgium; email: fabio.belloni@ec.europa.eu

Abstract

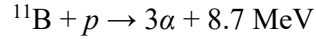
The $^{11}\text{B}(p,\alpha)2\alpha$ fusion reaction is particularly attractive for energy production purposes because of its aneutronic character and the absence of radioactive species among reactants and products. Its exploitation in the thermonuclear regime, however, appears to be prohibitive due to the low reactivity of the H-¹¹B fuel at temperatures up to 100 keV. A fusion chain sustained by elastic collisions between the α particles and fuel ions, this way scattered to suprathermal energies, has been proposed as a possible route to overcome this limitation. Based on a simple model, this work investigates the reproduction process in an infinite, non-degenerate H-¹¹B plasma, in a wide range of densities and temperatures which are of interest for laser-driven experiments ($10^{24} \lesssim n_e \lesssim 10^{28} \text{ cm}^{-3}$, $T_e \lesssim 100 \text{ keV}$, $T_i \sim 1 \text{ keV}$). In particular, cross section data for the α - p scattering which include the nuclear interaction have been used. The multiplication factor, k_∞ , increases markedly with electron temperature and less significantly with plasma density. However, even at the highest temperature and density considered, and despite a more than twofold increase by the inclusion of the nuclear scattering, k_∞ turns out to be of the order of 10^{-2} only. In general, values of k_∞ very close to 1 are needed in a confined scheme to enhance the suprathermal-to-thermonuclear energy yield by factors of up to $10^3 \div 10^4$.

Keywords

proton-boron fusion; $H^{11}B$ fuel; advanced fusion fuels; fusion chain reaction; avalanche $p-^{11}B$ fusion; suprathermal ion; $p-\alpha$ scattering

1. Introduction

The *advanced fusion fuel* (Dawson, 1981) based on a H-¹¹B mixture would exploit the reaction



which is particularly attractive as it involves only abundant and stable isotopes in the reactants, and no neutron in the reaction products. The reaction cross section shows a main, wide resonance at 612 keV in the CM system (Fig. 1a), with a maximum value of 1.4 b (Sikora and Weller, 2016). A second, narrow resonance at lower energy (147 keV) peaks to about 0.1 b. Summed over the three reaction channels – the low-BR ¹²C* direct breakup and the sequential decays via ⁸Be_{gs} or ⁸Be* (Becker *et al.*, 1987) – the energy spectrum of the generated α particles is a continuum which extends up to about 6.7 MeV in the lab, for a 675 keV incoming proton. The spectrum is strongly peaked around 4 MeV (Stave *et al.*, 2011).

A major drawback of H¹¹B fuel is due to the fact that the reaction cross section results in a much lower reactivity compared to conventional DT fuel, at the temperatures currently achievable in magnetically or inertially confined plasmas (of the order of 10 keV); Fig. 1b. This issue poses tremendous challenges to the feasibility of p -¹¹B fusion. Nevertheless, the fact that three charged, massive, energetic particles are produced in the reaction, suggests that the fusion yield could effectively be enhanced by a non-thermal effect induced by those particles, which is the elastic scattering of fuel ions to energies corresponding to the highest values of the fusion cross section (Brueckner and Brysk, 1973; Moreau, 1977). While thermalizing, some of the ions in these showers can undergo further fusion, eventually setting a chain reaction up. As a matter of fact, the fusion-born α 's can easily be stopped in the plasma, especially at very high densities. At those densities, moreover, the α 's tend to lose energy mostly to plasma ions rather than to electrons. This is certainly true in degenerate conditions (Gryzinski, 1958; Son

and Fisch, 2004) and, away from degeneracy, e.g. for $T_e \gtrsim T_i/10$ when $T_i \gtrsim 150$ keV and the boron-to-hydrogen ion concentration is lower than 50% (Levush and Cuperman, 1982).

In an infinite, homogeneous H¹¹B plasma, an α particle emitted at a certain energy $E_{\alpha,0}$ is characterised by the multiplication (or reproduction) factor $k_\alpha(E_{\alpha,0})$, which is the average number of secondary α -particles generated via suprathermal processes during its slowing down. For the purpose of this work, the multiplication factor in terms of fusion events, k_∞ , is well defined by the relation

$$k_\infty = \int k_\alpha(E_{\alpha,0})\varphi(E_{\alpha,0})dE_{\alpha,0} \quad (1)$$

where φ is the α spectral distribution normalised to 1. Each fusion event gives rise to new generations of events along a geometric progression. The number of events adds up, on average, to $1 + k_\infty + k_\infty^2 + \dots + k_\infty^l + \dots$, where l is the number of generations. Along these lines, it is not difficult to show that upon a thermonuclear rate per unit volume R , the time evolution of the cumulative number density of fusion events, $n_f(t)$, is given by

$$n_f(t) = \frac{R\tau_g}{1 - k_\infty} \left[\frac{t}{\tau_g} + \frac{k_\infty}{\ln k_\infty} \left(1 - k_\infty^{t/\tau_g} \right) \right] \quad (2)$$

where τ_g is the average period between two consecutive generations, and the initial condition $n_f(0) = 0$ has been assumed. Depending on whether i) $k_\infty < 1$, ii) $k_\infty = 1$, or iii) $k_\infty > 1$, n_f can respectively

- i) increase linearly with t , asymptotically to $Rt/(1 - k_\infty)$, for $t \rightarrow \infty$,
- ii) increase quadratically with t , as it reduces to $R(t + t^2/2\tau_g)$, or
- iii) diverge exponentially, with the growth rate $\ln k_\infty/\tau_g$.

It goes without saying that the capability to achieve a chain reaction with multiplicity $k_\infty \gtrsim 1$ would play a significant – if not indispensable – role in the possible exploitation of H^{11}B fusion for energy production purposes, especially under laser-driven schemes for plasma generation and confinement (Hora *et al.*, 2015, 2016, 2017).

Early k_α calculations by Moreau (1976, 1977), however, returned values of the order of 10^{-2} in a plasma with $100 \leq T_e \leq 300$ keV, $T_i = 0$, and Coulomb logarithm $\ln \Lambda = 5$. The boron-to-hydrogen ion concentration used is unclear (perhaps 8.9%, the optimum for thermonuclear ignition); moreover, only the Coulomb interaction was taken into account in the α -ion scattering, neglecting the nuclear (hadronic) one, which can instead turn out to be predominant, as we shall see. Recently, Hora *et al.* (2015, 2016) and Eliezer *et al.* (2016) have claimed evidence of the chain reaction in experiments at the Prague Asterix Laser System (PALS), Czech Republic, where an unprecedented fusion yield (4×10^8 α 's per laser pulse) had been achieved by irradiation of an H-enriched, B-doped Si target (Picciotto *et al.*, 2014; Margarone *et al.*, 2015). On the contrary, Shmatov (2016) and Belloni *et al.* (2018) have refuted this possibility on the basis of stopping power and α - p collision rate arguments. Lately, Eliezer and Martinez-Val (2020) have proposed the concept of a possible H^{11}B fusion reactor where the stopping power problem is circumvented by the application of an external electric field.

As it is evident, a systematic study of the chain reaction multiplicity in high-density H^{11}B plasma has been missing so far. Studies of this kind exist for DT fuel (e.g. Brueckner and Brysk, 1973; Peres and Shvarts, 1975; Afek *et al.*, 1978; Kumar *et al.*, 1986) and will briefly be outlined in Sect. 4. Prompted by recent theoretical and experimental advances in laser-driven p - ^{11}B fusion (Hora *et al.*, 2017; Giuffrida *et al.*, 2020), the advent of ultra-high-power (tens PW) laser systems as well as the growing interest of the scientific community in the potentiality of H^{11}B fuel for energy production (Rostoker *et al.*, 1997; Belyaev *et al.*, 2005; Labaune *et al.*, 2013; Cowen, 2013), this work reports an analysis of the multiplication process in a wide range

of plasma densities and temperatures which are of interest for current and future laser-based experiments. In particular, cross section data for the α - p scattering which include the nuclear interaction have been used. The aspiration is that results and conclusions can help inform the choice of parameters and the development of techniques in future experiments, with a view to maximising multiplication effects.

2. Theory

We assume a two-temperature (T_e, T_i), H¹¹B plasma with n_j ions per unit volume (the subscript j stands for p or B); the density ratio n_B/n_p is denoted by γ . Indicating by $E_{j,0}$ the energy of an ion just after the scattering by an α particle, we will consider as suprathermal those secondary ions for which $E_{j,0} \gg T_i$. In this limit, the number of ions of the species j scattered into the energy interval $(E_{j,0}, E_{j,0} + dE_{j,0})$ through the path length dx of the α particle is given by

$$d^2N_j = n_j \sigma_s(E_\alpha, E_{j,0}) dE_{j,0} dx \quad (3)$$

where σ_s is the differential scattering cross section. The spectral distribution of these ions through the entire path length of the α particle is then

$$\frac{dN_j}{dE_{j,0}}(E_{j,0}; E_{\alpha,0}) = n_j \int_{\frac{3}{2}T_i}^{E_{\alpha,0}} \sigma_s(E_\alpha, E_{j,0}) \left(\frac{dE_\alpha}{dx}\right)^{-1} dE_\alpha \quad (4)$$

where dE_α/dx is the stopping power of the α particle (taken as a positive quantity). For pure Coulomb scattering, σ_s is given by the well-known Rutherford cross section, σ_R , which reads, in terms of $E_{j,0}$, as

$$\sigma_R(E_\alpha, E_{j,0}) = \frac{\pi(z_\alpha z_j e^2)^2 m_\alpha}{E_\alpha E_{j,0}^2 m_j} H(E_{j,0}^{max} - E_{j,0}) \quad (5)$$

where the z 's are particle electric charges in units of the elementary charge e , the m 's are particle masses, H is the Heaviside step function, and the endpoint energy $E_{j,0}^{max}$ is given, from basic kinematics, by

$$E_{j,0}^{max} = \eta_{\alpha j} E_\alpha \quad (6)$$

with $\eta_{\alpha j} = 4m_\alpha m_j / (m_\alpha + m_j)^2$.

Denoting by $k_{\alpha j}$ the contribution to k_α of the suprathermal population of the species j , it is straightforward to see that for an α particle of energy $E_{\alpha,0}$, the spectrum of $k_{\alpha j}$ over $E_{j,0}$ is linked to the spectrum of N_j by

$$\frac{dk_{\alpha j}}{dE_{j,0}}(E_{j,0}; E_{\alpha,0}) = 3 P_j(E_{j,0}) \frac{dN_j}{dE_{j,0}}(E_{j,0}; E_{\alpha,0}) \quad (7)$$

where P_j is the fusion probability of the ion throughout its thermalisation, and the factor of 3 is the number of α 's per fusion event. $k_{\alpha j}(E_{\alpha,0})$ is calculated by numerical integration of Eq. (7) over $E_{j,0}$. In turn, k_α is calculated by summing over the contribution of each ion species, i.e.

$$k_\alpha(E_{\alpha,0}) = k_{\alpha p}(E_{\alpha,0}) + k_{\alpha B}(E_{\alpha,0}) \quad (8)$$

Finally, k_∞ is calculated from $k_\alpha(E_{\alpha,0})$ through Eq. (1). By the same way, it is also meaningful to calculate the spectrum $dk_{\infty,j}/dE_{j,0}$ from $dk_{\alpha j}/dE_{j,0}$.

Concerning the fusion probability in Eq. (7), it is easy to show (e.g. Giuffrida *et al.*, 2020) that in the cold-ion approximation for the target species, and for $P_j \ll 1$ (which is our case, see Sect. 3), the following relation holds

$$P_{p(B)}(E_{p(B),0}) = n_{B(p)} \int_0^{E_{p(B),0}} \sigma_f(E_{CM}) \left(\frac{dE_{p(B)}}{dx} \right)^{-1} dE_{p(B)} \quad (9)$$

where dE_j/dx is the stopping power, σ_f is the fusion cross section, and E_{CM} is the CM energy of the p - ^{11}B system, i.e.

$$E_{CM} = \frac{m_{B(p)}}{m_p + m_B} E_{p(B)} \quad (10)$$

Calculations of the abovementioned quantities have been performed in conditions relevant to laser-driven fusion plasmas and are reviewed in Sect. 3. In computations, we have adopted the following input data or models and considerations.

α spectrum, $\varphi(E_{\alpha,0})$

By the sake of simplicity, we have used the crude two-group approximation according to which, on average, one α particle is emitted at energy $E_{\alpha,I} = 1$ MeV and the other two at $E_{\alpha,II} = 4$ MeV (Stave *et al.*, 2011). Consequently, $\varphi(E_{\alpha,0})$ in Eq. (1) is given by

$$\varphi(E_{\alpha,0}) = \frac{1}{3} [\delta(E_{\alpha,0} - E_{\alpha,I}) + 2\delta(E_{\alpha,0} - E_{\alpha,II})] \quad (11)$$

where δ is the Dirac delta function.

Fusion cross section, σ_f

The analytic approximation of Nevins and Swain (2000) has been used below 3.5 MeV, and an interpolation of TENDL evaluated data (Koning *et al.*, 2019) at higher energies (Fig. 1a).

Elastic scattering cross section, σ_s

For the α - p scattering, evaluated cross section data have been interpolated from SigmaCalc (Gurbich, 2016). A comparison with σ_R is displayed in Fig. 2, which shows that the nuclear contribution dramatically increases the cross section, within a factor of 3 for $E_\alpha \lesssim 2$ MeV, up to a factor of 10 around 4 MeV and at high values of $E_{p,0}$, and by hundreds of times at progressively higher values of E_α and $E_{p,0}$. Nevertheless, for $E_\alpha > 4$ MeV and $E_{p,0} < 1$ MeV, a wide area exists where $\sigma_s/\sigma_R < 1$, which is an effect of the interference between the Coulomb and nuclear scattering amplitudes (Perkins and Cullen, 1981). For the α - ^{11}B scattering, the Rutherford cross section has been used as the higher Coulomb barrier makes the nuclear contribution negligible at the energies concerned.

Stopping powers, dE_α/dx and dE_j/dx

The Spitzer-Sivukhin model (Spitzer, 1956; Sivukhin, 1966) has been used, in the form for a multicomponent (electrons and ion species), two-temperature H^{11}B plasma detailed in Levush and Cuperman (1982). Earlier, this model had also been used by Moreau (1976, 1977) for slowdown calculations in high-density H^{11}B plasma. With a view to the subsequent discussion, it is worth recalling the form of the electronic stopping power in the expressions of dE_α/dx and dE_j/dx , i.e.

$$dE_{qe}/dx = n_e \ln \Lambda_{qe}(n_e, T_e) g_{qe}(E_q, T_e) \quad (12)$$

where the subscript q stands for α , p or B, and the functions $\ln\Lambda_{qe}$ and g_{qe} are given by Sivukhin (1966). Analogous formulas hold for the q - p and q - ^{11}B components of the stopping power.

Plasma electron density, n_e

With reference to Eqs. (4) and (9), it is useful to write the ion densities appearing therein in terms of the electron density, n_e , and γ , i.e.

$$n_p = n_e / (z_p + z_B \gamma) \quad (13a)$$

$$n_B = n_e \gamma / (z_p + z_B \gamma) \quad (13b)$$

Orders of magnitudes between 10^{24} and 10^{28} cm^{-3} have been considered for n_e . As a term of reference, for amorphous boron in STP conditions, $n_B = 1.3 \times 10^{23} \text{ cm}^{-3}$, hence $n_e = 6.5 \times 10^{23} \text{ cm}^{-3}$.

Boron-to-hydrogen ion concentration, γ

If one considers, by the sake of simplicity, only the electronic stopping power in the expressions of dE_α/dx and dE_j/dx [Eq. (12)], it is straightforward to note that the apparent linear dependence on n_e in Eqs. (4) and (9) actually cancels out, leaving factors which depend on γ according to Eqs. (13). This implies that Eq. (7) and derived quantities depend on γ through the overall factor $\gamma / (z_p + z_B \gamma)^2$, which has a maximum at $\gamma = 0.2$ for $z_p = 1$ and $z_B = 5$. In reality, the dependence of the multiplication factors on γ is obviously much more complicate because of the dependence on n_j of the ion-ion components of the stopping powers. The optimum γ has to be calculated numerically and depends, moreover, on the specific set of parameters entering the equations. Its value and the corresponding maximum values of k_α and k_∞ , however, are in general not dramatically affected, as shown in Sect. 3.

Temperatures, T_e and T_i

Minimising dE_α/dx and dE_j/dx in Eqs. (4) and (9), respectively, requires high values of both T_e and T_i in a classic (Maxwell-Boltzmann) plasma. As a precondition, one wants to deal with a fully ionized plasma in order to reduce the electronic component of the stopping power (Giuffrida *et al.*, 2020); accordingly, T_e should be much higher than the ionization energy of B^{4+} , which is 0.34 keV for the isolated ion (Lide, 2000) and less in high-density matter (More, 1993). Even when T_e is higher than the B^{4+} ionization energy, electrons can still be Fermi-degenerate at the high densities considered here. The Fermi energy E_F , which scales as $n_e^{2/3}$, has been plotted in Fig. 3 for reference. In view of further reducing the electronic stopping power, we have verified that in our density domain it is convenient to work at low degeneracy, e.g. at $T_e/E_F > 5$, compared to the fully degenerate case (Son and Fisch, 2004; Giuffrida *et al.*, 2020). Accordingly, at a given n_e , we have chosen to work with a classic plasma with $T_e > 5E_F$, a condition which in our case ensures both full ionization and low degeneracy. On the other hand, at a given T_e , the lower T_i the more effective is the suprathreshold energy transfer. Indeed, in the limit $T_i = 0$, all the scattered ions are obviously suprathreshold; moreover, from basic kinematics, the collisional energy transfer from the α particle to the ion occurs as long as the velocity of the former is higher than that of the latter. We have chosen to set $T_i = 1$ keV, which is a good compromise among the needs to reduce the ion-ion component of the stopping power, increase the α -to-ion energy partition, and ensure a suprathreshold spectrum as wide as possible ($T_i \ll E_{j,0} \leq E_{j,0}^{max}$). As a matter of fact, the contribution to $k_{\alpha p}$ of protons with $E_{p,0} < 10$ keV is absolutely negligible; see Sect. 3. Incidentally, in a low- T_i scheme the thermonuclear burn will be very modest and will just be used to seed the chain reaction, which is expected to provide most of the energy output. The choice of parameters $10^{24} \leq n_e \leq 10^{28} \text{ cm}^{-3}$, $T_i = 1$ keV, $\max[T_i, 5E_F(n_e)] \leq T_e \leq 100$ keV (Fig. 3) appears to be of interest for present and

future laser-driven experiments where hot electrons are generated in shocked or inertially compressed targets; see e.g. the recent experiment of Giuffrida *et al.* (2020) on a shocked hydrogen-rich boron nitride target, where $n_e \sim 10^{24} \text{ cm}^{-3}$ and $T_e \sim T_i \sim 1 \text{ keV}$ have been estimated.

3. Results

The ^{11}B -ion contribution to k_α in Eq. (8) turns out to be in any case much smaller than that of the proton, by a factor of at least 100, as we have verified by direct computation for values of $E_{\alpha,0}$ up to 10 MeV. Accordingly, explicit results for suprathreshold ^{11}B ions will not be reported in the followings. The physical reasons for the negligible role of ^{11}B recoils in the multiplication process will be outlined in Sect. 4. In the present Section, focus is made on the results of calculations for $P_p(E_{p,0})$, $dN_p/dE_{p,0}$, $dk_{\alpha p}/dE_{p,0}$, $dk_{\infty,p}/dE_{p,0}$, $k_{\alpha p}(E_{\alpha,0})$, and k_∞ .

The fusion probability of Eq. (9) has been plotted in Fig. 4 as a function of proton energy for representative values of n_e and T_e , with $T_i = 1 \text{ keV}$ and $\gamma = 0.2$. The shape of the curves resembles the main features of σ_f . The curves, in particular, exhibit marked knees at energies around the main cross section resonances. Further, the fusion probability becomes negligibly small below 100 keV. Within our domain of parameters, values of P_p of the order of 10^{-3} are attained at proton energies between approximately 400 and 500 keV. The fusion probability is enhanced more effectively by increasing T_e rather than n_e (the curves at 10^{25} and 10^{26} cm^{-3} are almost indistinguishable); furthermore, the T_e -driven enhancement is amplified by proton energy. While the dependence on T_e is entirely due to the stopping power in Eq. (9), the slight dependence on n_e results from its quasi cancellation in the product between n_B and $(dE_p/dx)^{-1}$, as discussed in Sect. 2.

The spectral analysis of scattered protons and multiplication factors is provided in Fig. 5. In panel a), $dN_p/dE_{p,0}$ has been plotted according to Eq. (4), for the two reference values of $E_{\alpha,0}$ (viz. $E_{\alpha,I}$ and $E_{\alpha,II}$) and the elastic cross sections σ_s and σ_R , respectively. First, one notes that the spectrum endpoint energies, as given by Eq. (6), are quite high, approaching 600 keV in the case of $E_{\alpha,I}$ and overcoming 2 MeV in the case of $E_{\alpha,II}$. Secondly, at the given values of $E_{\alpha,0}$, the trend of the curves corresponding to σ_s and σ_R is similar. Nevertheless, at values of $E_{p,0}$ of the order of 10 keV and beyond, one notes that the yield of scattered protons is significantly higher when the nuclear interaction is taken into account. At intermediate energies, of the order of 100 keV, the difference reduces significantly. At energies of the order of 1 MeV, the scattered yield is again enhanced by the nuclear interaction. Such ‘‘oscillation’’ in this proton energy range is basically due to the interference between the scattering amplitudes of the nuclear and Coulomb potentials, as mentioned in Sect. 2. In panel b), $dk_{\alpha p}/dE_{p,0}$ has been plotted according to Eq. (7), for the two reference values of $E_{\alpha,0}$ and the same set of parameters indicated in panel a). The distribution $dk_{\infty,p}/dE_{p,0}$ resulting from the α spectrum of Eq. (11) is also shown. Despite the increasing yield of scattered protons at low $E_{p,0}$, it is immediate to recognise that the contribution to $k_{\alpha p}$ and $k_{\infty,p}$ from protons with $E_{p,0} \lesssim 100$ keV is negligible. This is obviously due to the extremely low fusion probability at those energies. One can also notice that the contribution to $k_{\infty,p}$ of the low-energy α 's (blue curve) is rather limited.

A detailed analysis of the behaviour of $k_{\alpha p}(E_{\alpha,0})$ with T_e and n_e is shown in Fig. 6. In panel a), curves have been generated for three different values of T_e (10, 50 and 100 keV), keeping n_e fixed at 10^{26} cm⁻³. As a term of comparison, a curve based only on the Rutherford α - p scattering has been calculated at $T_e = 50$ keV. In panel b), n_e has been varied by 1-decade steps from 10^{24} to 10^{28} cm⁻³ while keeping T_e fixed at 100 keV. In all cases, the curves quickly

drop below $E_{\alpha,0} \simeq 2$ MeV. Above 4 MeV, their shape is approximately linear in the semi-log plot, meaning an exponential increase with $E_{\alpha,0}$. A fit with a function of the form $k_{\alpha p} \propto \exp(aE_{\alpha,0})$ on the curves of panel b) returns $a \simeq 0.45 \text{ MeV}^{-1}$ for $4 \leq E_{\alpha,0} \leq 10$ MeV, meaning that $k_{\alpha p}$ increases by a factor of about 2.5 each time $E_{\alpha,0}$ increases by 2 MeV.

At a given $E_{\alpha,0}$, $k_{\alpha p}$ increases with both T_e and n_e , as expected from stopping power considerations. The slope of the straight portion of the curves in Fig. 6 slightly increases with T_e , whereas it is unaffected by variations of n_e . In the latter case, the spacing between adjacent curves increases with regularity upon tenfold increments of n_e . However, the logarithmic sensitivity of $k_{\alpha p}$ to n_e is very limited; for instance, $\partial \ln k_{\alpha p} / \partial \ln n_e < 0.12$ at $T_e = 100$ keV, whereas for $n_e = 10^{26} \text{ cm}^{-3}$, $\partial \ln k_{\alpha p} / \partial \ln T_e$ approximately ranges from 2.3 at $T_e = 10$ keV to 1.8 at $T_e = 100$ keV. We also remark the effect of the use of σ_s instead of σ_R in the α - p scattering. In Fig. 6a, the gap of the respective curves at $T_e = 50$ keV progressively increases with $E_{\alpha,0}$, resulting in a value of $k_{\alpha p}$ which e.g., at $E_{\alpha,0} = 10$ MeV, is about 8 times higher when the nuclear interaction is taken into account. Despite this and the abovementioned favourable features, even at the highest values of $E_{\alpha,0}$, T_e and n_e considered in this work, $k_{\alpha p}$ remains significantly lower than 1.

Finally, the dependence on γ of $k_{\alpha p}(E_{\alpha,I})$, $k_{\alpha p}(E_{\alpha,II})$ and the resulting k_{∞} is shown in Fig. 7, in the range $0 \leq \gamma \leq 1$ and for the most multiplication-effective (viz the highest) values of n_e and T_e explored in this work. As it is obvious, the curves vanish for $\gamma \rightarrow 0$ (too few ^{11}B ions for the fusion reaction to occur) and decrease smoothly to 0 for $\gamma > 1$ (too few protons available for scattering). In between, a maximum occurs at values of γ which depend on E_{α} and are however not far from 0.2, the value argued in Sect. 2 and used in the calculations above. More importantly, the differences in $k_{\alpha p}(E_{\alpha,I})$, $k_{\alpha p}(E_{\alpha,II})$ and k_{∞} between the case $\gamma = 0.2$

and the respective optimal γ 's are limited to the order of 10%. We remark that in the conditions of Fig. 7, the peak value for our estimate of k_∞ is only of the order of 10^{-2} .

4. Discussion

As anticipated, it is instructive remarking the physical reasons behind the very modest impact of suprathreshold ^{11}B ions on the multiplication process. It is already evident from Eq. (10) for the p - ^{11}B CM energy in the fixed-target reaction that the fusion probability of suprathreshold ^{11}B ions is much smaller than that of protons, at the same particle energy. Indeed, E_{CM} is suppressed by a factor m_p/m_B , resulting in very low values of σ_f in Eq. (9). Moreover, at the same particle energy, dE_B/dx is larger than dE_p/dx , which still depresses the integrand in Eq. (9). On the opposite, at given $E_{\alpha,0}$ and ion energy, $dN_B/dE_{B,0}$ tends to be larger than $dN_p/dE_{p,0}$, by a factor $(z_B/z_p)^2 m_p/m_B = 2.3$ when $\sigma_s = \sigma_R$ is assumed in Eq. (4). Also, the ^{11}B suprathreshold spectrum is slightly wider than the proton one, since $E_{B,0}^{max}/E_{p,0}^{max} = \eta_{\alpha B}/\eta_{\alpha p} = 1.2$. Nevertheless, the net result from Eq. (7) is that the ^{11}B contribution to k_α in Eq. (8) is in any case much smaller than the proton one.

Though the findings of Sect. 3 prevent the possibility of achieving the chain reaction in realistic conditions, it is of utmost importance to study how and how much a weak multiplication regime, i.e. when $k_\infty < 1$ (and especially $k_\infty \ll 1$), can enhance the pure thermonuclear burn. In this respect, the ratio of the energy per unit volume produced during the confinement time τ_c , \mathcal{E} , to the energy stemming from the sole thermonuclear burn, \mathcal{E}_{th} , is just $n_f(\tau_c)/R\tau_c$, where $n_f(t)$ is given by Eq. (2). We prefer to study this ratio in the form of the fractional increment $I \equiv (\mathcal{E} - \mathcal{E}_{th})/\mathcal{E}_{th}$, which is equivalent to the suprathreshold-to-

thermonuclear energy yield, $\mathcal{E}_{st}/\mathcal{E}_{th}$, since the suprathreshold energy component, \mathcal{E}_{st} , is obviously $\mathcal{E} - \mathcal{E}_{th}$. Explicitly,

$$I(k_\infty) = \frac{\mathcal{E}_{st}}{\mathcal{E}_{th}}(k_\infty) = \frac{k_\infty}{1 - k_\infty} \left(1 + \frac{\tau_\alpha}{\tau_c} \frac{1 - k_\infty^{\tau_c/\tau_\alpha}}{\ln k_\infty} \right) \quad (14)$$

where τ_α is the spectrum-averaged thermalisation time of the α 's, and we have used the fact that $\tau_g \approx \tau_\alpha$. Indeed, if one estimates τ_g as the average extinction time of the α -induced recoil shower, then $\tau_g^2 \approx \tau_\alpha^2 + \tau_p^2$, where τ_p is the spectrum-averaged thermalisation time of the secondary protons; τ_p is obviously longer than the average thermalisation time of B ions, but much shorter than τ_α .

One immediately notes that I depends on the ratio τ_c/τ_α as a parameter. At the plasma densities considered here and for $T_e \sim 5E_F$, τ_α generally turns out to be of the order of 1 ps or lower. With $\tau_c \sim 1$ ns, τ_c/τ_α can then reach the order of 10^3 or 10^4 . Notice that for a self-sustaining chain reaction (i.e. $k_\infty \geq 1$), τ_c/τ_α represents the maximum possible number of α -particle generations within the time τ_c .

Plots of I as a function of k_∞ are shown in Fig. 8, for several orders of magnitude of τ_c/τ_α and $k_\infty < 1$. In the limit $\tau_c/\tau_\alpha \rightarrow \infty$, Eq. (14) yields the asymptotic behaviour $I \sim k_\infty/(1 - k_\infty)$ which, being independent of τ_c/τ_α , explains the saturation of the curves observed at high values of the parameter. For $k_\infty \ll 1$, one recognises the approximate scaling $I \sim k_\infty$ in Fig. 8. This means that in the plasma conditions investigated in this work, the burn enhancement due to the multiplication is of the order of 1% at most.

In the limit $k_\infty \rightarrow 1$, Eq. (14) yields $I \rightarrow (1/2) \tau_c/\tau_\alpha$. This opens the possibility of very large increments in the energy output (and consequently, high fusion gains); however, at high

τ_c/τ_α , I raises steeply when $k_\infty \rightarrow 1$, so that k_∞ has to lie very close to 1 to allow increments of the order of τ_c/τ_α being approached (e.g. $I \approx 0.37 \tau_c/\tau_\alpha$ when $1 - k_\infty = \tau_\alpha/\tau_c$, for $\tau_c/\tau_\alpha \gg 1$).

To summarise, our parametric analysis has shown that k_∞ increases markedly with T_e and less significantly with n_e , with the optimum γ lying between 0.2 and 0.4. The achievable fusion energy is further enhanced by the ratio τ_c/τ_α . In the weak chain, however, the enhancement is quite limited moving from $\tau_c/\tau_\alpha \sim 10$ to $\tau_c/\tau_\alpha \sim 100$ while $k_\infty \lesssim 0.5$, and negligible beyond $\tau_c/\tau_\alpha \sim 100$ while $k_\infty \lesssim 0.9$. We note, moreover, that there is a trade-off between the requirements for rising T_e up on the one hand, and keeping τ_c/τ_α sufficiently large on the other hand, since τ_α also increases with T_e (on the contrary, τ_α decreases with n_e as $1/n_e \ln \Lambda$). For typical confinement times, however, values of τ_c/τ_α larger than at least 10 appear to be always ensured.

We conclude this Section by making contact with previous representative findings for DT fuel. Peres and Shvarts (1975) have shown that a chain reaction via elastic recoils can proceed in a cold infinite DT plasma at densities above 8.4×10^{27} ions/cm³. The optimum isotopic ratio is $n_D/n_T = 0.72$. In the analysis, they have also considered recoil-induced DD and TT fusion reactions and the scattering by their products. The main contributor to the chain reaction turns out to be the DT-born 14.1 MeV neutron, while the 3.5 MeV α particle contributes only a few percent. Indeed, if the neutron is disregarded, the medium is not critical even at 10^{29} ions/cm³, the highest density considered by the authors. This observation is of interest for inertial confinement experiments, where the neutron can easily escape the compressed pellet. For a finite-temperature, infinite plasma, however, Afek *et al.* (1978) have found lower critical densities; for instance, 1.0×10^{27} ions/cm³ at $T_e = T_i = 14$ keV and $n_D/n_T = 0.64$. For the finite-temperature, finite-size case, Kumar *et al.* (1986) have estimated

an upper bound of 0.5 for the suprathreshold fusion probability associated to the DT neutron in a pellet compressed to a thickness (ρr) of a few g/cm², at a density of 6.0×10^{25} ions/cm³ (roughly 1000 times the solid density), $T_e = T_i = 40$ keV, and $n_D/n_T = 1$. We conclude that the suprathreshold contribution to the fusion yield is substantially lower in H¹¹B fuel compared to DT fuel, in similar plasma conditions and for cases of practical interest.

5. Conclusion

We have investigated the possibility of a fusion chain reaction via α -recoiled ions in high-density, non-degenerate H¹¹B plasma, under conditions which are of interest for laser-driven experiments ($10^{24} \lesssim n_e \lesssim 10^{28}$ cm⁻³, $T_e \lesssim 100$ keV, $T_i \sim 1$ keV). On the basis of a simple model, the multiplication factor for individual fusion events (k_∞) has been estimated in terms of the energy-dependent multiplication factor for individual α particles (k_α), by averaging over the α emission spectrum. A spectral analysis of the suprathreshold proton population and of the multiplication factors is also reported.

We have found that the contribution of suprathreshold ¹¹B ions to k_α and k_∞ is of the order of 1% only. In the case of the scattered proton, the complete elastic cross section, accounting also for the nuclear interaction, must be used in calculations. For instance, the value of k_α for the most probable α emission energy (about 4 MeV) turns out to be more than twice that found for a pure Coulomb scattering. The spectral analysis shows that only protons with recoil energies higher than or comparable to 100 keV contribute to the multiplication factors. This important limitation is essentially due to the drop of the fusion probability at lower energies.

The parametric analysis shows that k_α increases with both T_e and n_e , though it is much more sensitive to T_e . The optimum γ lies between 0.2 and 0.4. In general, k_α quickly drops

below $E_{\alpha,0} \simeq 2$ MeV, while it increases nearly exponentially above 4 MeV, up to at least 10 MeV, the highest α energy considered in this work. Even for the highest values of n_e and T_e considered, k_α (hence, k_∞) remain significantly lower than 1; $k_\alpha = 0.2$ for $E_{\alpha,0} = 10$ MeV, and $k_\infty \approx 0.01$. While $k_\infty \lesssim 0.3$, the fractional increment in the energy output relative to the thermonuclear burn scales linearly with k_∞ , being practically insensitive to the parameter τ_c/τ_α and remaining, therefore, quite limited. On the contrary, for $k_\infty \rightarrow 1$, the burn enhancement approaches the order of magnitude of τ_c/τ_α , which can easily be made as large as 10^3 or 10^4 in experiments.

Increasing k_∞ above the order of 10^{-2} , however, appears problematic in realistic laser-driven plasma conditions, meaning those presently achievable or likely to be achieved in the near future. One notes, moreover, that k_∞ in H^{11}B fuel is substantially lower than in DT fuel, *ceteris paribus*. Novel ideas are needed in order to exploit the full potential of suprathreshold multiplication in H^{11}B fuel. For instance, several authors (Belyaev *et al.*, 2005; Picciotto *et al.*, 2014; Giuffrida *et al.*, 2020) have reported α spectra shifted towards higher energies (up to 10 MeV) in laser-driven $p\text{-}^{11}\text{B}$ fusion experiments. Giuffrida *et al.* have ascribed this phenomenon to the acceleration of the fusion-born α 's by the same laser-induced electric field which accelerates the protons to MeV energies. With a proper choice of target characteristics and laser parameters, such an effect could represent an excellent means to exploit the nearly exponential increase of k_α at high α energy.

Acknowledgements

The author wishes to thank many of the participants in the 1st Discussion Workshop on Proton-Boron Fusion, 5 June 2020 (held remotely because of the Covid-19 outbreak), for debating the subject of this work during and after the event. The valuable support of D. Ostojić is also

gratefully acknowledged. All views expressed herein are entirely of the author and do not, in any way, engage his institution.

References

- Afek, Y., Dar, A., Peres, A., Ron, A., Shachar, R. and Shvarts, D. (1978). The fusion of suprathermal ions in a dense plasma. *J. Phys. D: Appl. Phys.* **11**, 2171-2173.
- Becker, H.W., Rolfs, C. and Trautvetter, H.P. (1987). Low-Energy Cross Sections for $^{11}\text{B}(p, 3\alpha)$. *Z. Phys. A - Atomic Nuclei* **327**, 341-355.
- Belloni, F., Margarone, D., Picciotto, A., Schillaci, F. and Giuffrida, L. (2018). On the enhancement of $p\text{-}^{11}\text{B}$ fusion reaction rate in laser-driven plasma by $\alpha \rightarrow p$ collisional energy transfer. *Phys. Plasmas* **25**, 020701.
- Belyaev, V.S., Matafonov, A.P., Vinogradov, V.I., Krainov, V.P., Lisitsa, V.S., Roussetski, A.S., Ignatyev, G.N. and Andrianov, V.P. (2005). Observation of neutronless fusion reactions in picosecond laser plasmas, *Phys. Rev. E* **72**, 026406.
- Bosch, H.-S. and Hale, G.M. (1992). Improved formulas for fusion cross-sections and thermal reactivities. *Nucl. Fusion* **32**, 611-632.
- Brueckner, K.A. and Brysk, H. (1973). Fast Charged Particle Reactions in a Plasma. *J. Plasma Phys.* **10**, 141-147.
- Cowen, R. (2013). Two-laser boron fusion lights the way to radiation-free energy. *Nature*, doi:10.1038/nature.2013.13914.
- Dawson, J.M. (1981). Advanced fusion reactors. In *Fusion* (Teller, E., Ed.), Vol. 1, Part B, pp. 453-502. New York: Academic Press.
- Eliezer, S., Hora, H., Korn, G., Nissim, N. and Martinez Val, J.M. (2016). Avalanche proton-boron fusion based on elastic nuclear collisions. *Phys. Plasmas* **23**, 050704.

- Eliezer, S. and Martinez-Val, J.M. (2020). A novel fusion reactor with chain reactions for proton-boron11. *Laser Part. Beams* **38**, 1-6.
- Giuffrida, L. *et al.* (2020). High-current stream of energetic α particles from laser-driven proton-boron fusion. *Phys. Rev. E* **101**, 013204.
- Gryzinski, M. (1958). Fusion Chain Reaction - Chain Reaction with Charged Particles. *Phys. Rev.* **111**, 900-905.
- Gurbich, A.F. (2016). SigmaCalc recent development and present status of the evaluated cross-sections for IBA. *Nucl. Instrum. Methods Phys. Res., B* **371**, 27-32.
- Hora, H., Lalouis, P., Giuffrida, L., Margarone, D., Korn, G., Eliezer, S., Miley, G.H., Moustazis, S. and Mourou, G. (2015). Petawatt laser pulses for proton-boron high gain fusion with avalanche reactions excluding problems of nuclear radiation. *Proc. SPIE* **9515**, 951518.
- Hora, H. *et al.* (2016). Avalanche boron fusion by laser picosecond block ignition with magnetic trapping for clean and economic reactor. *High Power Laser Sci. Eng.* **4**, e35.
- Hora, H. *et al.* (2017). Road map to clean energy using laser beam ignition of boron-hydrogen fusion. *Laser Part. Beams* **35**, 730-740.
- Koning, A.J., Rochman, D., Sublet, J., Dzysiuk, N., Fleming, M. and van der Marck, S. (2019). TENDL: Complete Nuclear Data Library for Innovative Nuclear Science and Technology. *Nucl. Data Sheets* **155**, 1-55.
- Kumar, A., Ligou, J.P. and Nicli, S.B. (1986). Nuclear scattering and suprathreshold fusion. *Fusion Sci. Technol.* **12**, 476-487.
- Labaune, C., Baccou, C., Depierreux, S., Goyon, C., Loisel, G., Yahia, V. and Rafelski, J. (2013). Fusion reactions initiated by laser-accelerated particle beams in a laser-produced plasma. *Nat. Commun.* **4**, 2506.

- Levush, B. and Cuperman, S. (1982). On the potentiality of the proton-boron fuel for inertially confined fusion. *Nucl. Fusion* **22**, 1519-1525.
- Lide, D.R., Ed. (2000). *Chemical Rubber Company handbook of chemistry and physics*. Boca Raton: CRC Press, 81st edition.
- Margarone, D. *et al.* (2015). Advanced scheme for high-yield laser driven nuclear reactions. *Plasma Phys. Control. Fusion* **57**, 014030.
- More, R.M. (1993). Atomic physics in dense plasmas. In *Nuclear Fusion by Inertial Confinement* (Velarde, G., Ronen, Y., Martinez Val, J.M., Eds.), pp. 151-170. Boca Raton: CRC Press.
- Moreau, D.C. (1976). Potentiality of the Proton-Boron Fuel for Controlled Thermonuclear Fusion. Thesis 1277-T, Department of Aerospace and Mechanical Sciences, Princeton University.
- Moreau, D.C. (1977). Potentiality of the proton-boron fuel for controlled thermonuclear fusion. *Nucl. Fusion* **17**, 13-20.
- Nevins, W.M. and Swain, R. (2000). The thermonuclear fusion rate coefficient for p-¹¹B reactions. *Nucl. Fusion* **40**, 865-872 .
- Peres, A. and Shvarts, D. (1975). Fusion chain reaction – a chain reaction with charged particles. *Nucl. Fusion* **15**, 687-692.
- Perkins, S.T. and Cullen, D.E. (1981). Elastic Nuclear Plus Interference Cross Sections for Light-Charged Particles. *Nucl. Sci. Eng.* **77**, 20-39.
- Picciotto, A. *et al.* (2014). Boron-Proton Nuclear-Fusion Enhancement Induced in Boron-Doped Silicon Targets by Low-Contrast Pulsed Laser. *Phys. Rev. X* **4**, 031030.

Rostoker, N., Binderbauer, M.W. and Monkhorst, H.J. (1997). Colliding Beam Fusion Reactor. *Science* **278**, 1419-1422.

Shmatov, M.L. (2016). Comment on “Avalanche proton-boron fusion based on elastic nuclear collisions”. *Phys. Plasmas* **23**, 094703.

Sikora, M.H. and Weller, H.R. (2016). A New Evaluation of the $^{11}\text{B}(p,\alpha)\alpha$ Reaction Rates. *J. Fusion Energ.* **35**, 538–543.

Sivukhin, D.V. (1966). Coulomb collisions in a fully ionized plasma. In *Reviews of Plasma Physics* (Leontovich, M.A., Ed.), Vol. 4, p. 93. New York: Consultants Bureau.

Son, S. and Fisch, N.J. (2004). Aneutronic fusion in a degenerate plasma. *Phys. Lett. A* **329**, 76-82.

Spitzer, L. (1956). *Physics of Fully Ionized Gases*. New York: Interscience Publishers, Inc.

Stave, S., Ahmed, M.W., France III, R.H., Henshaw, S.S., Müller, B., Perdue, B.A., Prior, R.M., Spraker, M.C. and Weller, H.R. (2011). Understanding the $^{11}\text{B}(p,\alpha)\alpha$ reaction at the 0.675 MeV resonance. *Phys. Lett. B* **696**, 26-29.

Figure captions

Fig. 1. a) p - ^{11}B fusion cross section as a function of the CM energy, based on the analytic approximation of Nevins and Swain (2000) below 3.5 MeV and, above, on TENDL evaluated data. b) Reactivity as a function of ion temperature for H^{11}B fuel and, as a term of comparison, DT fuel. Plots are based on the analytic approximations of Nevins and Swain (2000) and Bosch and Hale (1992), respectively.

Fig. 2. Logarithmic contour plot of the ratio σ_s/σ_R in the $(E_\alpha, E_{p,0})$ plane, with the boundary given by Eq. (6).

Fig. 3. The (n_e, T_e) plane vs. Fermi degeneracy. Regions are shadowed according to the degree of degeneracy; the higher the darker the greytone. The white region is that investigated in this work.

Fig. 4. Proton fusion probability as a function of the incident energy, for different representative values of n_e and T_e .

Fig. 5. Spectral analysis of scattered protons (a) and multiplication factors (b) for α particles of initial energies $E_{\alpha,I}$ and $E_{\alpha,II}$. The values of n_e , T_e , T_i and γ indicated in panel a) have been used for calculations. Curves in panel a) are given for both the scattering cross sections σ_s and σ_R .

Fig. 6. α -particle multiplication factor via suprathermal protons as a function of the initial energy, for different values of T_e at a fixed n_e (a), and of n_e at a fixed T_e (b). In a), T_e values (in keV) are indicated next to the curves; as a term of comparison, a curve based only on the Rutherford α - p scattering (dashed line) has been generated at $T_e = 50$ keV.

Fig. 7. Multiplication factors $k_{\alpha p}$ and k_{∞} as a function of the boron-to-hydrogen ion concentration. Calculations are based on the two representative α -particle energies $E_{\alpha,I}$ and $E_{\alpha,II}$, and the indicated values of n_e , T_e and T_i .

Fig. 8. Suprathermal-to-thermonuclear energy ratio by the effect of a weak chain reaction, plotted as a function of k_{∞} for several orders of magnitude of the parameter τ_c/τ_{α} .

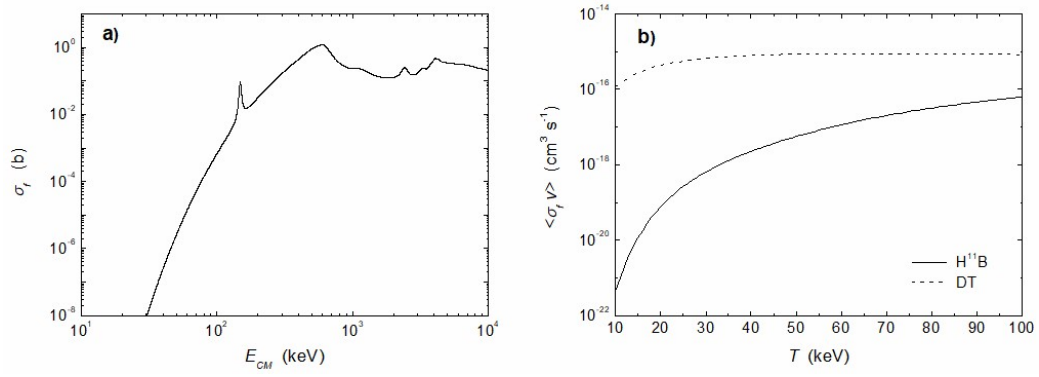


Fig. 1 – F. Belloni

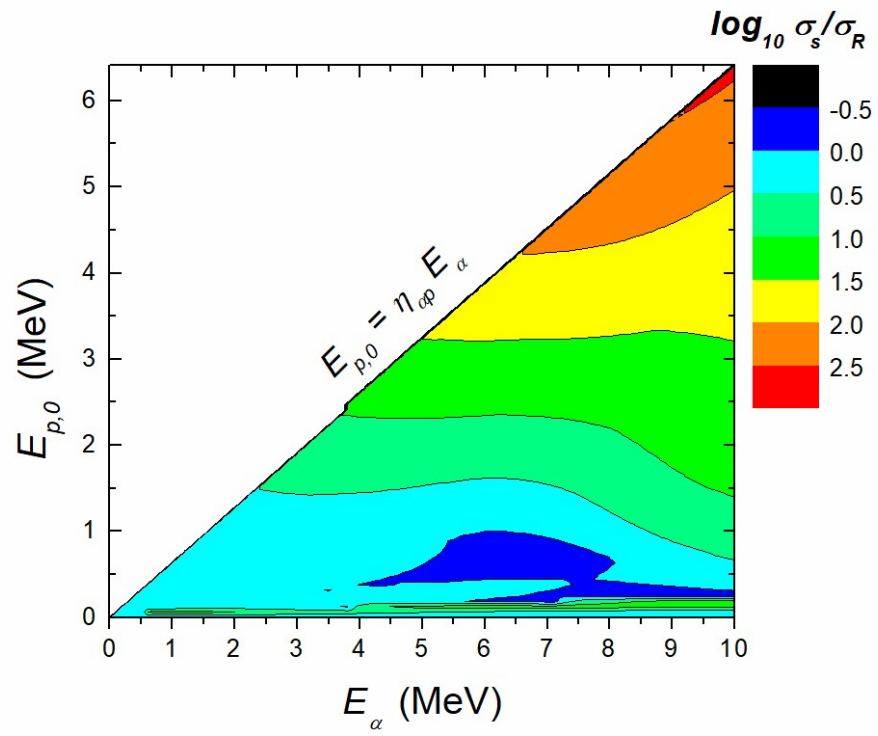


Fig. 2 – F. Belloni

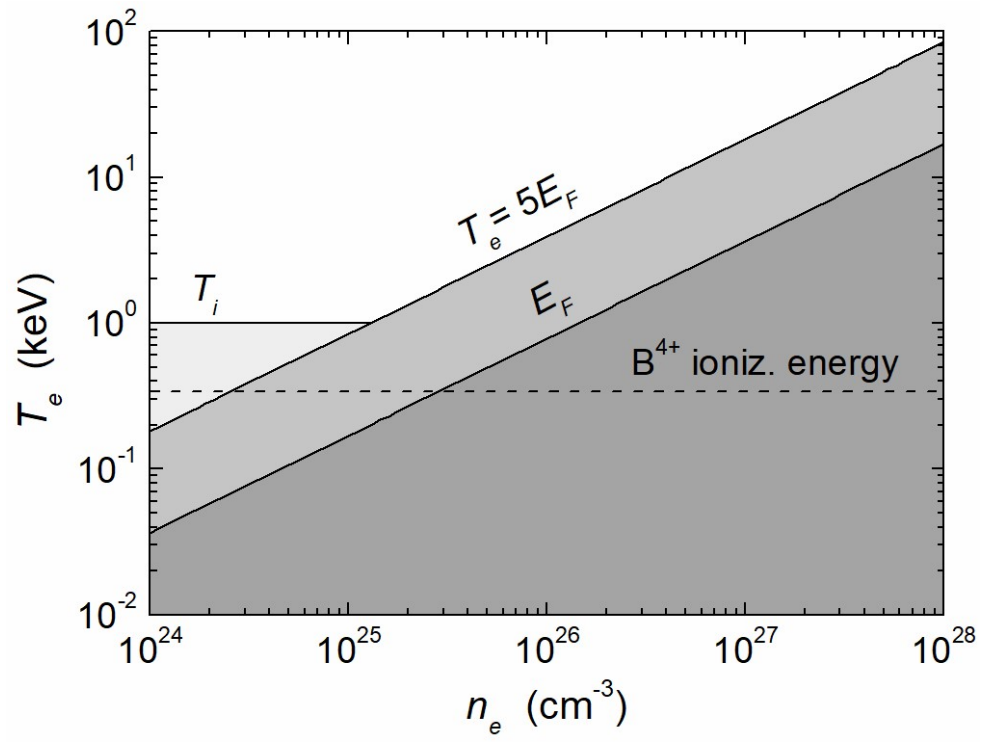


Fig. 3 – F. Belloni

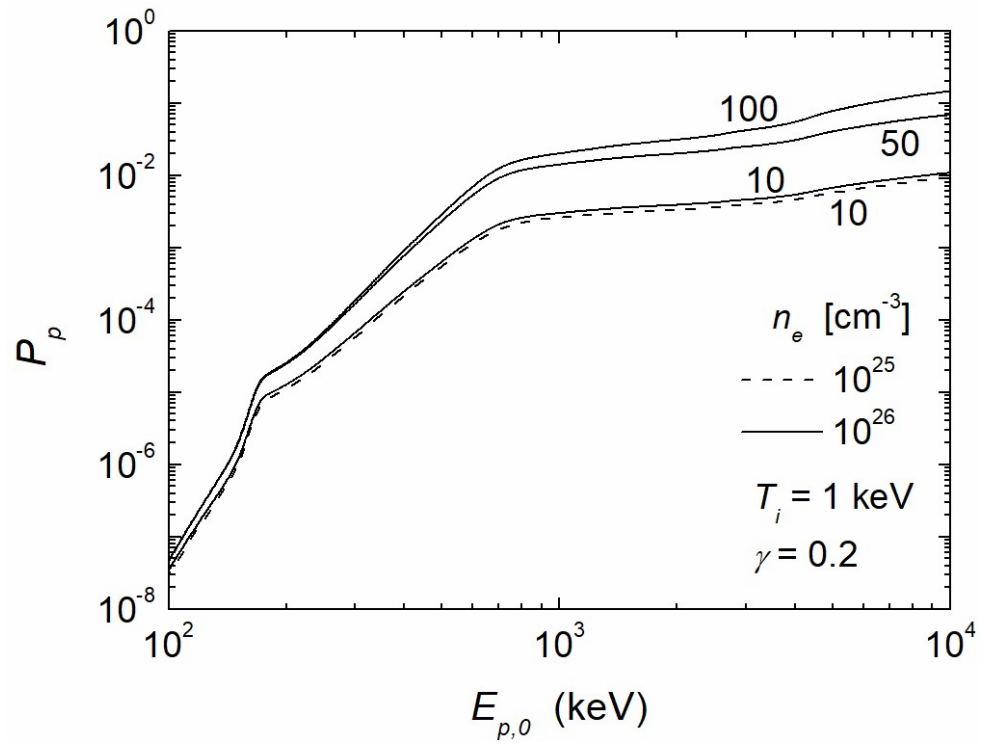


Fig. 4 – F. Belloni

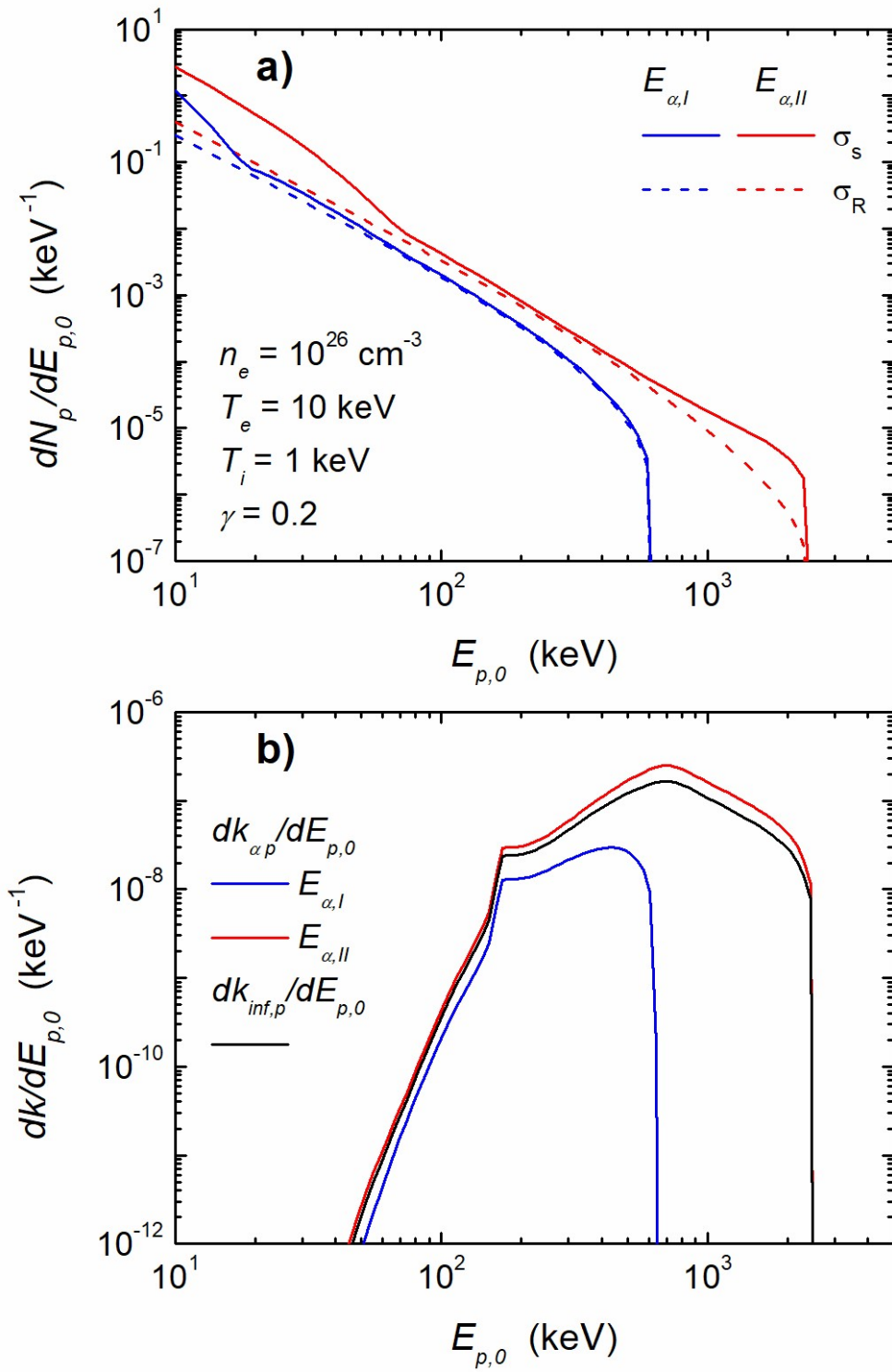


Fig. 5 – F. Belloni

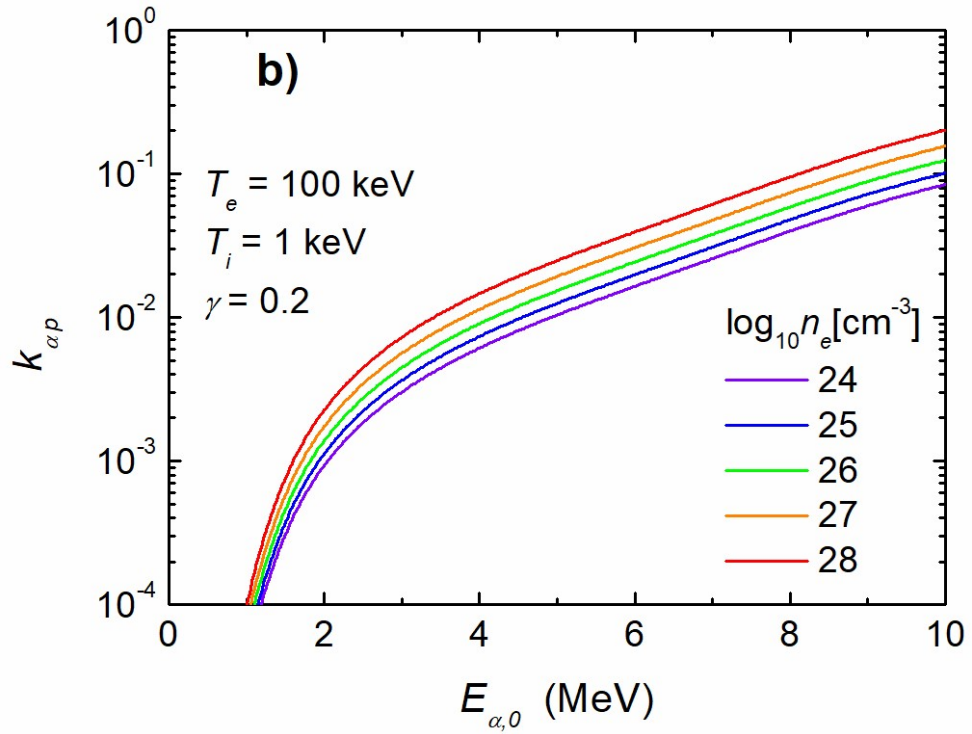
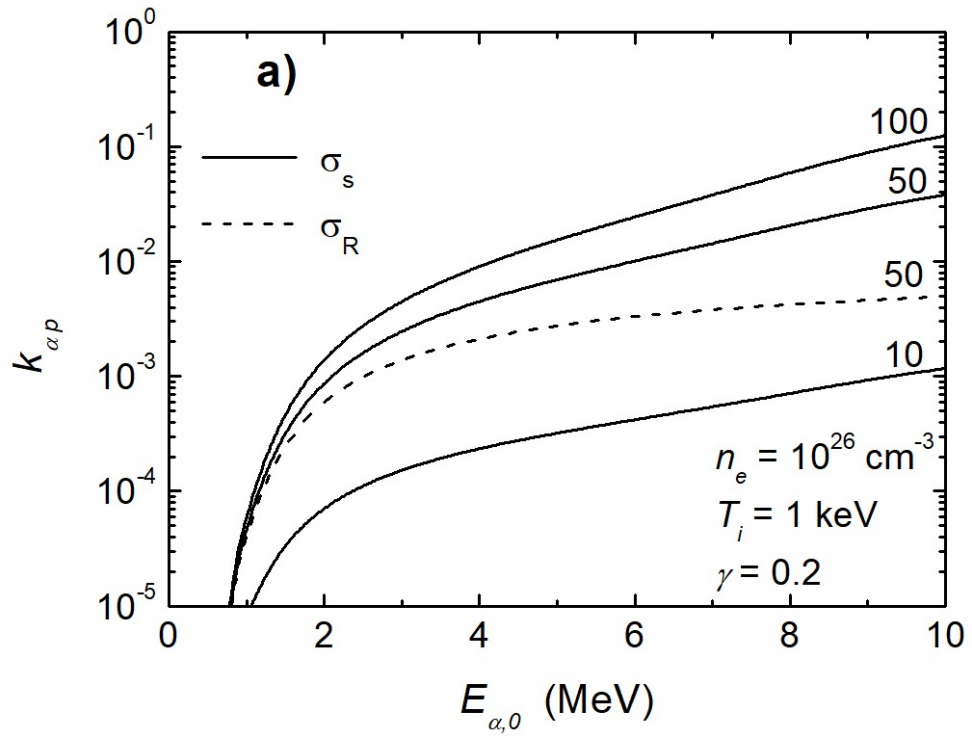


Fig. 6 – F. Belloni

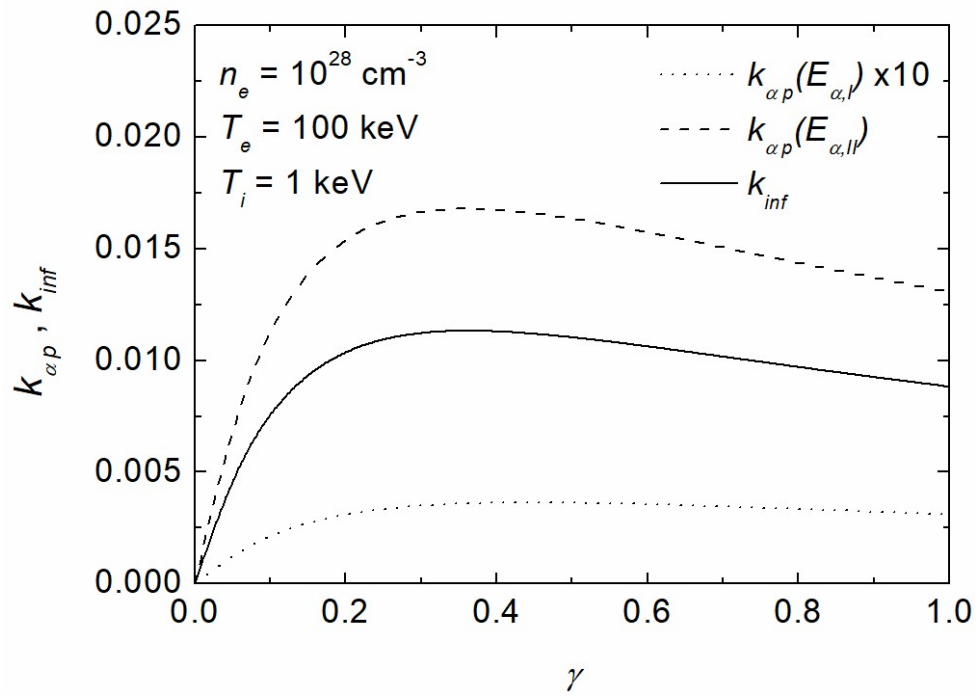


Fig. 7 – F. Belloni

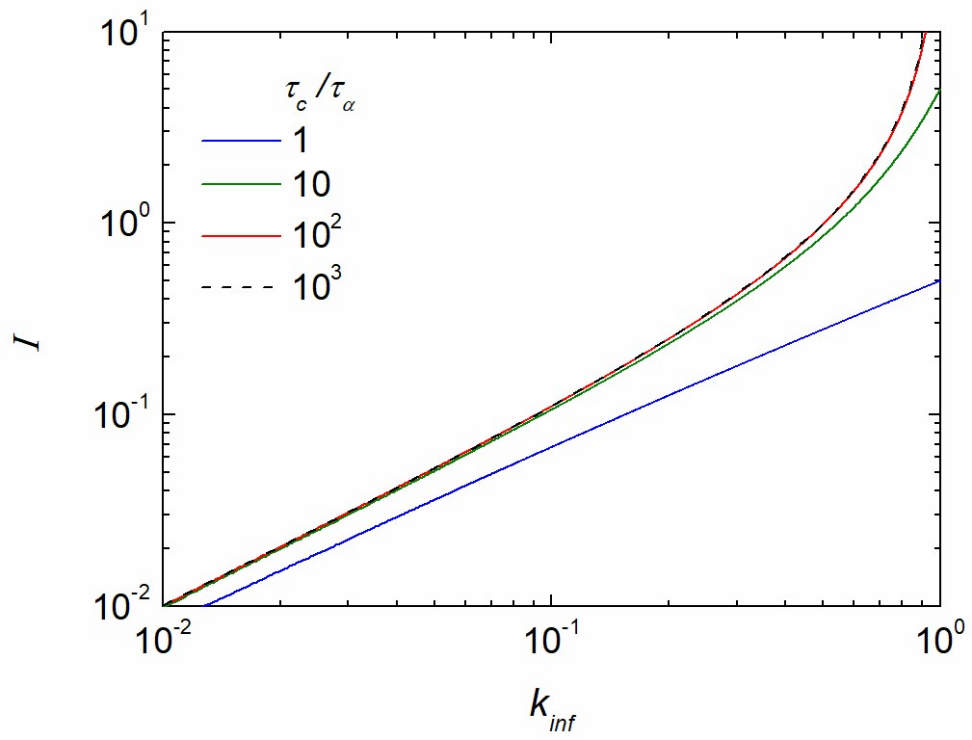


Fig. 8 – F. Belloni